AJNR

MR imaging of various oxidation states of intracellular and extracellular hemoglobin.

P A Janick, D B Hackney, R I Grossman and T Asakura

AJNR Am J Neuroradiol 1991, 12 (5) 891-897
http://www.ajnr.org/content/12/5/891

MR Imaging of Various Oxidation States of Intracellular and Extracellular Hemoglobin

Peter A. Janick[1]
David B. Hackney[1]
Robert I. Grossman[1]
Toshio Asakura[2]

The in vitro behavior of various states of hemoglobin was examined over a wide range of concentrations. Solutions of increasing concentrations of oxyhemoglobin displayed significant increases in T1 and T2 relaxation rates that were insensitive to pH values between 6.0 and 6.9. Bovine serum albumin, which displayed a relaxation behavior nearly identical to that of oxyhemoglobin, was used to normalize for the protein concentration of the deoxyhemoglobin and methemoglobin samples. Concentrated protein solutions with increasing proportions of deoxyhemoglobin yielded little change in the T1 relaxation rate. In these samples, however, the T2 relaxation rate displayed a parabolic dependence on the concentration of intracellular deoxyhemoglobin paralleling the inhomogeneity of the sample; this was not observed with extracellular deoxyhemoglobin. Similar T2 relaxation behavior was observed for intracellular methemoglobin, except that the magnitude of the T2 shortening was smaller than that for deoxyhemoglobin. The magnitude of the T2 shortening was pH dependent, roughly paralleling the change in the equilibrium between the high-spin acid form of methemoglobin and the low-spin basic form of methemoglobin. Marked increase in the T1 relaxation rate is observed with increasing concentrations of methemoglobin, again with greater relaxation enhancement at lower pH.

The results of our study emphasize the importance of normalizing for protein concentration when assessing the effects of paramagnetic forms of hemoglobin.

***AJNR* 12:891–897, September/October 1991**

The MR appearance of intracranial hemorrhage displays a characteristic evolution over time [1, 2]. Acutew intracerebral hematomas are isointense on short TR/short TE images and markedly hypointense on long TR/long TE and T2*-weighted images at high field. On the basis of the in vitro findings of Thulborn et al. [3], Gomori et al. [1, 4] concluded that the latter observation was caused by susceptibility effects due to intracellular deoxyhemoglobin (DeoxyHb). A more recent study [5] has challenged this assertion and related the profound hypointensity seen on long TR/long TE images to clotting proteins. With time, peripheral hyperintensity observed around hematomas on short TR/short TE images progresses centrally. The initial marked hypointensity observed on long TR/long TE images evolves to hyperintensity on long TR/long TE images long after the hematoma has become completely hyperintense on short TR/short TE images. The development of hyperintensity on short TR/short TE images has been ascribed to oxidation of DeoxyHb to methemoglobin (MetHb) [1, 6]. The transition from hypointensity on long TR/long TE images to hyperintensity on these sequences in subacute hematomas has been ascribed by Gomori et al. [1, 4] to lysis of MetHb containing red cells to yield free MetHb. In the chronic phase, much of the hematoma is resorbed, but residual hypointensity is observed owing to hemosiderin that is much more profound on long TR/long TE and T2* images than on short TR/short TE images [1].

In this study, we examined the in vitro behavior of DeoxyHb, MetHb, and oxyhemoglobin (HbO_2) over a wide range of concentrations to determine the

Received July 17, 1990; revision requested November 11, 1990; revision received February 25, 1991; accepted April 21, 1991.

[1] Department of Radiology, Hospital of the University of Pennsylvania, Philadelphia, PA 19104. Address reprint requests to R. I. Grossman.

[2] Department of Hematology, Hospital of the University of Pennsylvania, Philadelphia, PA 19104.

0195-6108/91/1205-0891

contributions of protein, susceptibility, and proton-electron dipole-dipole (PEDD) interactions to the MR signal intensity of hematomas. A high concentration of protein contributes significantly to the signal hyperintensity relative to water on short TR/short TE images and signal hypointensity relative to water on long TR/long TE images. However, these two MR phenomena are influenced more by PEDD interaction and susceptibility effects.

Materials and Methods

Human red cells from outdated blood bank blood were washed in saline and concentrated by centrifugation at 5000 rpm for 10 min to a hematocrit (Hct) of about 90%. Intracellular HbO_2 was prepared by swirling the washed packed RBCs to ensure complete oxygenation. Intracellular MetHb was produced by 1.5:1 volume/volume incubation of the packed RBCs with 2% sodium nitrite for 5 min followed by centrifugation and four washings with saline. DeoxyHb was produced by the addition of sodium dithionite (8 mg/ml). Concentrated bovine serum albumin (BSA) (Sigma Chemical Co., St. Louis, MO) was reconstituted at a concentration of 34 g/dl in saline (equivalent protein concentration to Hct = 90%). Extracellular hemoglobin was prepared by two cycles of freezing and thawing of the packed RBCs. The oxidation state of the hemoglobin was monitored spectrophotometrically. Determination of hemoglobin concentration was performed by bubbling diluted aliquots of the MetHb or HbO_2 with carbon monoxide gas and adding a crystal of sodium dithionite to prepare carboxyhemoglobin, followed by spectrophotometric determination of the optical density at 569 nm ($E = 13{,}000^{M-1}$). With this method, the concentration of extracellular hemoglobin was about 5 mmol/l. (Note that Hct = 90% corresponds to a protein concentration of 34 g/dl and a hemoglobin concentration of 5.2 mmol/l.) The pH of the DeoxyHb samples was 6.6. The pH of HbO_2 samples was 6.9, while the pH of the MetHb samples was 6.8. Samples of HbO_2 and MetHb were also adjusted to pH = 6.0 with hydrochloric acid. This was performed to ensure complete conversion of the MetHb to the acidic, high-spin form (pK = 7.7) [7].

MR imaging was performed on a standard 1.5-T Signa clinical scanner (General Electric Medical Systems, Milwaukee, WI) by using spin-echo sequences designed to yield T1-weighted, 600–1500/20 (TR/TE), and T2-weighted, 3000/30,60,90,120, images. Samples of HbO_2, BSA, and MetHb were imaged in Ping-Pong balls to minimize susceptibility effects due to container shape. DeoxyHb samples were studied in syringes to maintain anaerobiosis. T1 and T2 calculations were performed via region-of-interest determinations using the standard Signa system software.

Results

HbO_2

Various concentrations of HbO_2 diluted in saline were imaged; the results are summarized in Figure 1. Since the ferrous heme–oxygen complex is diamagnetic, these findings reflect the diamagnetic effects of the apohemoglobin protein molecule. It is clear from Figure 1 that these protein effects are not insignificant. It is also clear that there is little difference between intra- and extracellular HbO_2. Furthermore, the HbO_2 samples were insensitive to pH between pH values of 6.0 and 6.9. The T1 and T2 relaxation rates for extracellular HbO_2 and BSA are shown in Figure 2. The differences in the relaxation rate between the two proteins are minimal. The slopes of the linear fits to the data are presented in Table 1.

DeoxyHb

Varying the concentration of DeoxyHb affects the protein concentration as well as the concentration of the paramag-

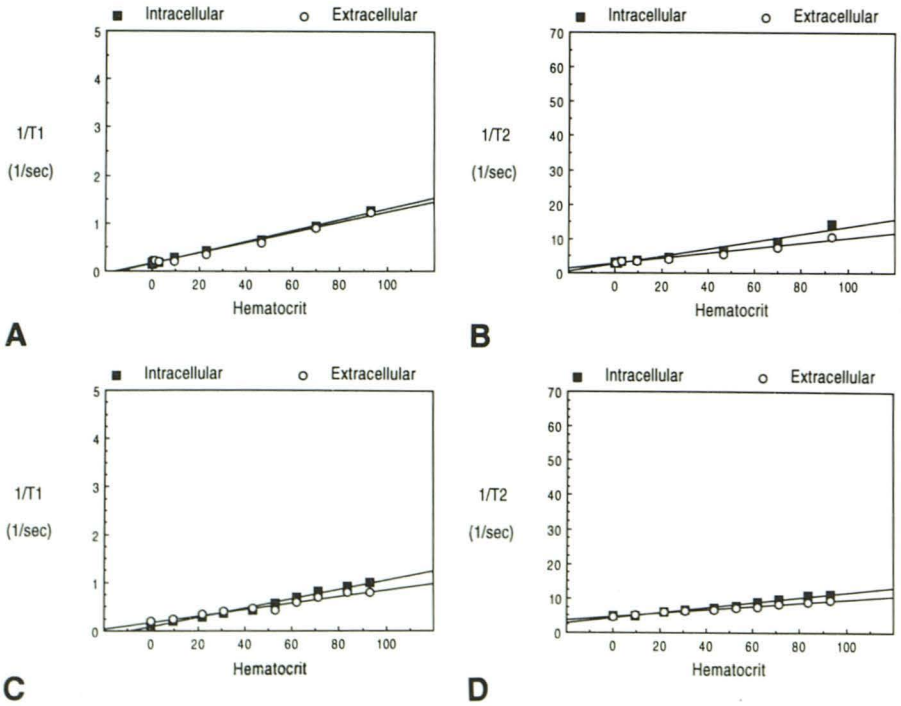

Fig. 1.—T1 and T2 relaxation rates of oxyhemoglobin as a function of concentration. Concentrated intra- or extracellular oxyhemoglobin was diluted with saline to varying concentrations and imaged by using spin sequences described in text. Calculated relaxation times, 1/T1 or 1/T2, are plotted as a function of hemoglobin concentration expressed as hematocrit (or equivalent hematocrit in the case of extracellular oxyhemoglobin).
***A*, 1/T1 at pH = 6.9.**
***B*, 1/T2 at pH = 6.9.**
***C*, 1/T1 at pH = 6.0.**
***D*, 1/T2 at pH = 6.0.**

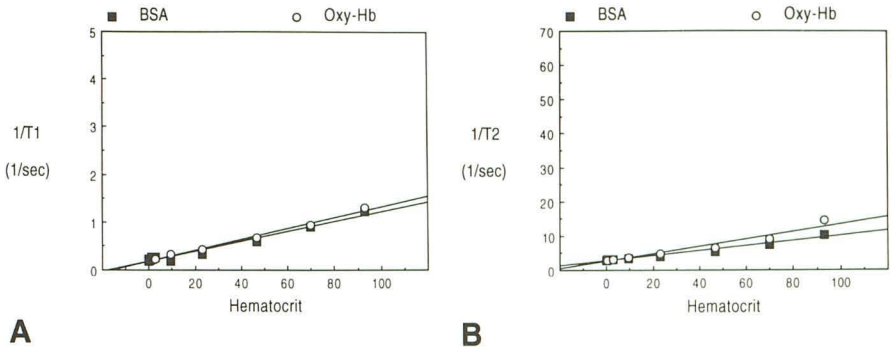

Fig. 2.—T1 and T2 relaxation rates of extracellular oxyhemoglobin (Oxy-Hb) and bovine serum albumin (BSA) as a function of concentration. Concentrated BSA (34 mg/dl) or extracellular oxyhemoglobin was diluted with saline to varying concentrations and imaged by using spin sequences described in text. Calculated relaxation times, 1/T1 or 1/T2, are plotted as a function of protein concentration expressed as the corresponding hematocrit (e.g., hematocrit for 19 mg/dl is 50%). pH was 6.9.
***A*, 1/T1.**
***B*, 1/T2.**

TABLE 1: Slopes and Correlation Coefficients for Standard Linear Regressions Performed on Data

Solution	Slope × 10^{-2} (1/sec)		r^2	
	T1	T2	T1	T2
Oxyhemoglobin in saline (pH = 6.0)				
Intracellular	0.964	7.32	.982	.983
Extracellular	0.667	4.88	.964	.988
Oxyhemoglobin in saline (pH = 6.9)				
Intracellular	1.14	10.9	.995	.955
Extracellular	1.05	7.39	.975	.961
Bovine serum albumin in saline (pH = 6.9)	1.03	7.23	.964	.968
Methemoglobin in bovine serum albumin (pH = 6.0)				
Intracellular	3.11		.997	
Extracellular	2.54	1.86	.994	.611
Methemoglobin in bovine serum albumin (pH = 6.8)				
Intracellular	1.97		.995	
Deoxyhemoglobin in bovine serum albumin (pH = 6.6)				
Intracellular	0.202		.814	
Extracellular	−0.195	−0.393	.898	.968

netic heme. To isolate the paramagnetic effects of DeoxyHb, varying concentrations of DeoxyHb were prepared by using concentrated BSA as a diluent rather than saline. This produced samples with a constant protein concentration yet varying amounts of the paramagnetic Fe^{2+} heme. As shown in Figure 2, BSA and HbO_2 display nearly identical relaxation behavior, allowing the substitution. Figure 3A demonstrates that the T1 relaxation rate for intra- and extracellular DeoxyHb in BSA is virtually independent of the concentration of DeoxyHb. This confirms the absence of significant PEDD proton relaxation enhancement (PRE), as previously described [4].

The effects of DeoxyHb on the T2 relaxation rate are much more dramatic (Fig. 3B). As with the T1 relaxation rate, there is little change in the T2 relaxation rate with increasing concentration for extracellular DeoxyHb. This again demonstrates the small contribution to the T2 relaxation rate from PEDD interaction. However, for intracellular DeoxyHb, there are profound changes in the T2 relaxation rate with a strong dependence on Hct. Maximal T2 shortening is observed at an Hct approximating 50%. This effect diminishes at both high and low Hct values. Contributions to the T2 relaxation rate are additive, allowing deconvolution of the various contributions to the overall observed relaxation rate as follows:

$$1/T2_{\text{Intracellular DeoxyHb}} = 1/T2_{\text{protein}} + 1/T2_{\text{PEDD-PRE}} + 1/T2_{\text{inhomogeneity}}. \quad (1)$$

Since extracellular DeoxyHb is a homogeneous solution, its T2 relaxation rate should only have protein and PEDD-PRE contributions:

$$1/T2_{\text{Extracellular DeoxyHb}} = 1/T2_{\text{protein}} + 1/T2_{\text{PEDD-PRE}}. \quad (2)$$

Therefore, it follows that

$$1/T2_{\text{Inhomogeneity}} = 1/T2_{\text{Intracellular DeoxyHb}} - 1/T2_{\text{Extracellular DeoxyHb}}. \quad (3)$$

In Figure 3C, the T2 relaxation effects attributable to the inhomogeneity effect alone are compared with the combined T2 relaxation rates due to protein and PEDD-PRE. From these data, it is readily apparent that significant contributions to the T2 relaxation rate are produced even at Hct values of 10% or 90% that are as great or greater than the effects due to the protein and PEDD-PRE effects alone. The solid line in Figure 3C represents a measure of the inhomogeneity (Hct)(100 − Hct) of the intracellular DeoxyHb solution scaled to the maximal T2 relaxation rate at an Hct of about 50%.

MetHb

The relaxation behavior of intra- and extracellular MetHb as a function of Hct is presented in Figure 4. MetHb exists in both an acidic and a basic form with a pKa of 7.7 [7]. The ferric heme in the basic form is in the S = 1/2 low-spin state, while in the acidic form the heme assumes the high-spin S = 5/2 state. Thus, the magnetic behavior of MetHb is markedly dependent on pH, as a large difference in susceptibility exists between the two states. MetHb was studied at pH = 6, where only 2% of MetHb would be expected to be in the basic form, and at pH = 6.8, where 11% would be in the basic form.

The T1 relaxation rate for MetHb in BSA is shown in Figures 4A and 4B. Note that there is little difference in the relaxation rate between intra- and extracellular MetHb. Comparison between the T1 relaxation rates of MetHb and HbO_2 allows deconvolution of the relaxation rate attributable to the PEDD-PRE. Since

$$1/T1_{\text{Extracellular MetHb}} = 1/T1_{\text{protein}} + 1/T1_{\text{PEDD-PRE}} \quad (4)$$

and

$$1/T1_{\text{BSA}} = 1/T1_{\text{protein}},$$

then

$$1/T1_{PEDD\text{-}PRE} = 1/T1_{Extracellular\ MetHb} - 1/T1_{BSA}, \quad (5)$$

where $1/T1_{BSA}$ is the T1 relaxation rate for the Hct = 0 point in Figure 4A or 4B (BSA = 34 g/dl, equivalent to an Hct of 90%). Since

$$1/T1_{HbO_2} = 1/T1_{BSA} = 1/T1_{protein}, \quad (6)$$

the protein contribution to the T1 relaxation rate can be appreciated by plotting the data for HbO_2 in saline. As seen in Figures 4C and 4D, while the protein and PEDD-PRE contributions to the T1 relaxation rate are of the same order of magnitude, the PEDD-PRE effects are larger.

As with DeoxyHb, the contributions to the T2 relaxation rate of MetHb were investigated by imaging various concentrations of intra- and extracellular MetHb using a concentrated BSA solution as the diluent rather than saline. The overall relaxation rate for these two species as a function of Hct is given in Figures 5A and 5B. As seen by the minor rise in the T2 relaxation rate for extracellular MetHb as a function of Hct, the PEDD-PRE contribution to T2 relaxation is small. On the other hand, like DeoxyHb, the T2 relaxation rate of MetHb is markedly influenced by the inhomogeneity produced by the encapsulation of MetHb within the RBC. Again, the maximal increase in the T2 relaxation rate of intracellular MetHb is observed near an Hct of 50%. The maximal T2 relaxation rate at an Hct of about 50% at a pH of 6.8 is 83% of that at a pH of 6.0, consistent with the lesser proportion of the MetHb in the high-spin acid form. The T2 relaxation contribution of the inhomogeneity was calculated for intracellular MetHb in a fashion identical to that for intracellular DeoxyHb and is shown in Figure 5C. Again, significant inhomogeneity contributions to the T2 relaxation rate are observed at Hct values of 10% and 90%, as predicted (solid line calculated in a fashion identical to that for intracellular DeoxyHb in Fig. 3C).

Discussion

The hyperintensity observed in subacute hematomas on short TR/short TE images has been postulated [1, 6] to represent MetHb effects. Our results clearly show that MetHb, both in intra- and extracellular states, can produce the clinically observed hyperintensity on short TR/short TE images. This hyperintensity results from both contributions from the diamagnetic effects of the protein portion of the hemoglobin molecule and the PEDD-PRE effect of the high-spin ferric heme in MetHb. Deconvolution of the contributions to the T1 relaxation rate of MetHb shows that the PEDD-PRE effect is larger than the protein effect at intermediate Hct values (≈50%). With increasing protein concentration, the well-known progressive shortening of T1 is demonstrated [8, 9]. This effect has been ascribed to slowing of the rotational motion of water molecules due to binding and structuring of the water molecules immediately surrounding the protein molecule. Slowing of the rotational rate of the solvent water molecules has been shown to enhance longitudinal relaxation [10]. The magnitude of this effect is known to be dependent on the protein molecular weight [11]. Indeed, the relaxation behavior of HbO_2 (molecular weight = 64,450) is nearly identical to that of BSA (molecular weight = 66,000). For HbO_2 or DeoxyHb, only the protein effect makes significant contributions to the T1 relaxation rate and produces the hyperintensity relative to CSF observed clinically on short TR/short TE images.

The same rotational effects of increased protein concentration that cause the increase in the T1 relaxation rate of concentrated protein solutions also produce an increase in the T2 relaxation rate [10]. The T2 shortening properties of the high-spin Fe^{3+} heme, when normalized for protein concentration, are relatively minor compared with the protein-induced effects. The T2 shortening effects of the high-spin ferrous heme of DeoxyHb is even smaller, indicating an absence of PEDD-PRE effects. This can be rationalized on the

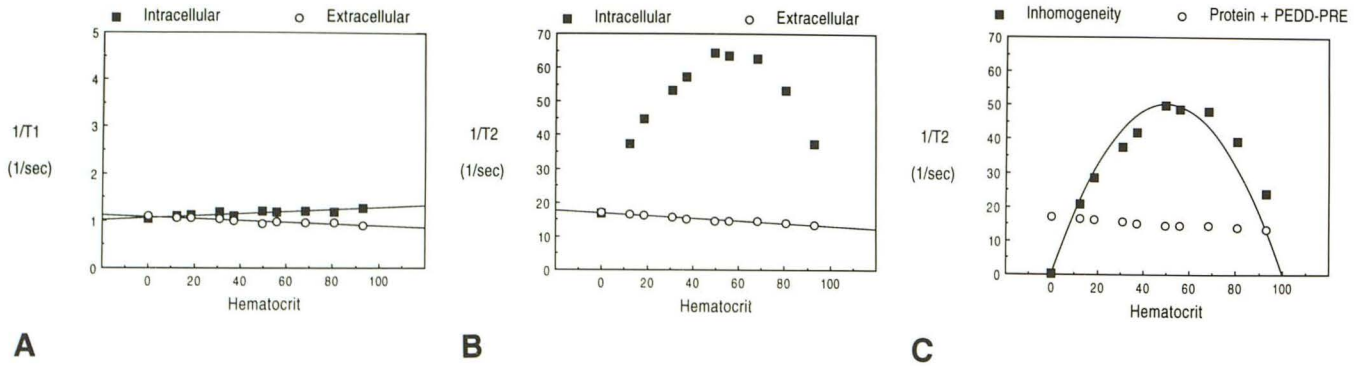

Fig. 3.—T1 and T2 relaxation rates of deoxyhemoglobin as a function of concentration. Concentrated intracellular or extracellular deoxyhemoglobin was diluted with bovine serum albumin to varying concentrations and imaged by using spin sequences described in text. Calculated relaxation times, 1/T1 or 1/T2, are plotted as a function of hemoglobin concentration expressed as hematocrit (or equivalent hematocrit in the case of extracellular deoxyhemoglobin).

***A*, 1/T1.**

***B*, 1/T2.**

***C*, Protein and proton-electron dipole-dipole proton relaxation enhancement (PEDD-PRE) contributions to 1/T2 as expressed by 1/T2 for extracellular deoxyhemoglobin (see equation 2 in text) and inhomogeneity contribution expressed by equation 3 in text. *Solid line* shows expected inhomogeneity contribution predicted by (hematocrit)(100 – hematocrit) scaled to maximal observed inhomogeneity contribution at a hematocrit of approximately 50%.**

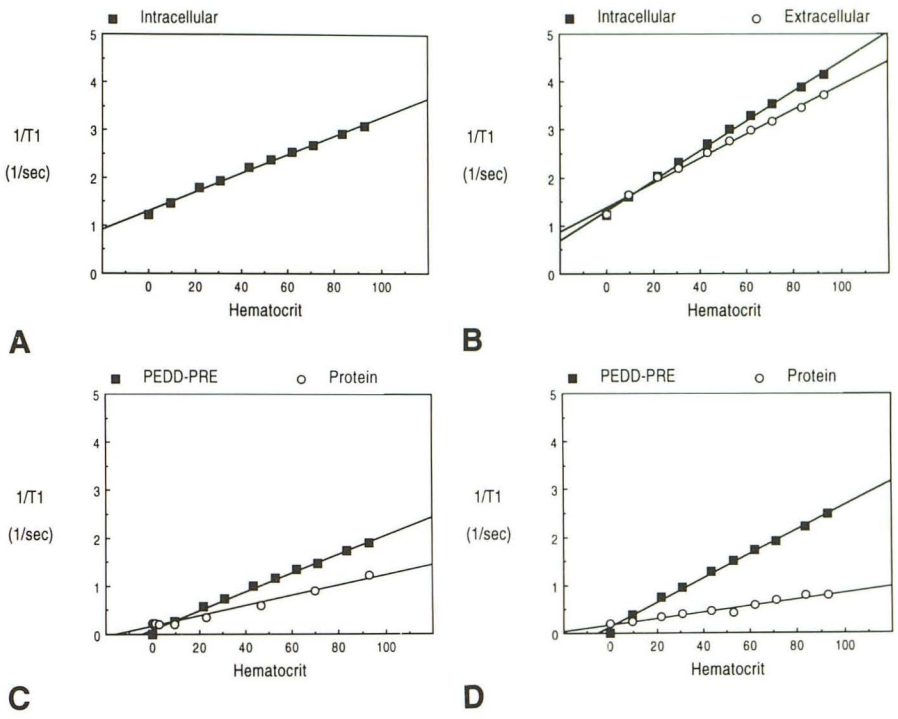

Fig. 4.—1/T1 relaxation rates of methemoglobin as a function of concentration. Concentrated intra- or extracellular methemoglobin was diluted with bovine serum albumin to varying concentrations and imaged by using spin sequences described in text. Calculated relaxation times are plotted as a function of hemoglobin concentration expressed as hematocrit (or equivalent hematocrit in the case of extracellular methemoglobin).

***A*, 1/T1 at pH = 6.8.**

***B*, 1/T1 at pH = 6.0.**

***C*, Protein contribution to 1/T1 as expressed by 1/T1 for extracellular oxyhemoglobin diluted in saline (see equation 6 in text) as plotted in Fig. 1 and proton-electron dipole-dipole proton relaxation enhancement (PEDD-PRE) contribution expressed by equation 5 at pH = 6.8.**

***D*, Same as *C* except at pH = 6.0.**

basis of an understanding of the structure of DeoxyHb. Conformational changes in the quartenary and tertiary structure of hemoglobin occur on conversion of HbO_2 to DeoxyHb, causing the histidine F8 ligand of the heme iron atom to be pulled away from the plane of the heme and off the perpendicular axis to the porphyrin ring. The displacement of the heme iron from the porphyrin ring bows the heme molecule, preventing water molecules from easily binding to the opposite side of the heme [12]. Thus, water molecules have difficulty approaching the heme within the 0.3 nm [13] required to produce significant PEDD-PRE.

The effect of encapsulating the DeoxyHb within the red cell, however, produces a profound change in the signal characteristics of DeoxyHb on long TR/long TE and gradient-refocused T2*-weighted images. Thulborn et al. [3] described increases in the T2 relaxation rate of intracellular DeoxyHb

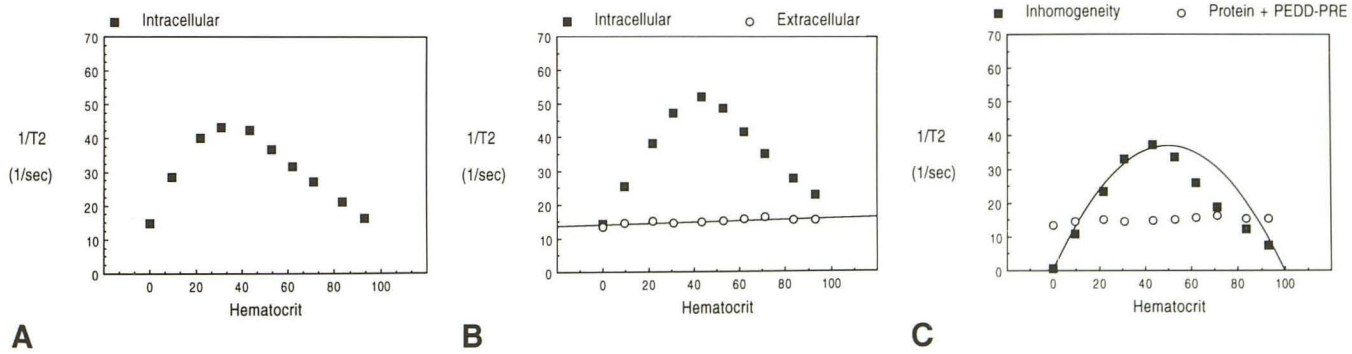

Fig. 5.—1/T2 relaxation rates of methemoglobin as a function of concentration. Concentrated intra- or extracellular oxyhemoglobin was diluted with bovine serum albumin to varying concentrations and imaged by using spin sequences described in the text. Calculated relaxation times are plotted as a function of hemoglobin concentration expressed as hematocrit (or equivalent hematocrit in the case of extracellular methemoglobin).

***A*, 1/T2 at pH = 6.8.**

***B*, 1/T2 at pH = 6.0.**

***C*, Protein and proton-electron dipole-dipole proton relaxation enhancement (PEDD-PRE) contributions to 1/T2 as expressed by 1/T2 for extracellular methemoglobin (see equation 2 in text) and inhomogeneity contribution expressed by equation 3 at pH = 6.0. *Solid line* shows expected inhomogeneity contribution predicted by (hematocrit)(100 – hematocrit) scaled to maximal observed inhomogeneity contribution at a hematocrit of approximately 50%.**

when compared with intracellular HbO_2 at fields of 1.9–11 T. They related this phenomenon to susceptibility effects resulting from local field inhomogeneity produced by the paramagnetic DeoxyHb within the red cell as was noted by other workers [14, 15]. Clark et al. [16] observed a linear relationship between Hct and T2 relaxation time for intracellular DeoxyHb. However, these workers used a Carr-Purcell-Meiboom-Gill (CPMG) spin sequence with $2\tau_{CPMG} = 2$ msec, which would greatly diminish the contribution of local field inhomogeneity effects to the T2 relaxation rate [4]. Gomori et al. [4] showed a similar effect with MetHb at a single point (Hct = 45%). Our results confirm the findings of Thulborn et al. [3] and correct for the changes due to protein concentration. It is clear that the susceptibility effects are substantial compared with the protein effects, especially at the maxima observed near Hct = 50%, as predicted by the degree of heterogeneity. Indeed, even at an Hct of 90%, corresponding to the approximate Hct of clot, the contribution of susceptibility would be predicted to be 36% of maximal, which for intracellular DeoxyHb is greater than that expected for the protein effects alone.

Similar results are observed with MetHb; however, the susceptibility effect would be expected to be larger than that for DeoxyHb, as the susceptibility effect is predicted to be proportional to $(n)(n + 2)$, where n is the number of unpaired electrons on the heme iron atom. Experimentally, however, this was not observed, as the maximal susceptibility effect for MetHb was slightly lower in magnitude than that observed for DeoxyHb. The added osmolarity of the extracellular solution due to the exogenously added sodium dithionite may significantly increase the intracellular concentration of the DeoxyHb and enhance T2 relaxation. Nevertheless, a significant susceptibility effect is still observed for intracellular MetHb, even at an Hct of 90%. The clinically observed variability in signal intensity of subacute hematomas on long TR/long TE sequences, therefore, can be explained on the basis of the relative proportions of intra- and extracellular MetHb and the attendant cellular-induced magnetic field gradients, particularly in the early stages of subacute hemorrhage. The observation that subacute hematomas become more hyperintense with time on long TR/long TE images thus would reflect lysis of the red cells to produce extracellular MetHb and the concomitant diminution of the susceptibility effects as the local field inhomogeneity is lost. With time, however, changes in protein concentration within the hematoma may become more important, particularly once all the red cells have lysed.

Hayman et al. [17] studied partially deoxygenated intra- and extracellular hemoglobin at 0.23 and 4.69 T. They reported a decrease in T2 with increasing hemoglobin concentration, which largely reflects nonspecific changes in protein concentration as the samples they used at high field were predominantly HbO_2 (oxygen saturation, 73%). Nonetheless, greater decreases in T2 were observed in their intracellular samples relative to extracellular samples, maximal at the Hct data point of 43%. In a second study [5], these workers studied clotted blood and experimental "clots" of coagulated fibrin free of red cells. They found hypointensity in DeoxyHb clots and the red cell–free clots, and therefore attributed the clinically observed hypointensity to the coagulation protein alone rather than to paramagnetic-induced susceptibility changes arising from the DeoxyHb. The hypointensity of their red cell-free clots may have been a function of the protein concentration of the clot itself, as they made no attempt to ensure that the fibrin matrix within the artificial red cell–free clot was at the same protein concentration as the fibrin matrix within the red cell–containing clot. Since about 90% of a clot would be expected to consist of the red cells, such a hypothesis would require that the signal of the clot be totally dominated by the remaining 10% or less of the clot due to the fibrin matrix. Furthermore, our data suggest that the DeoxyHb-containing red cells exert a profound influence on the observed signal intensity of clots. The hypointensity of the red cell–free clots on long TR/long TE images probably reflects the increased protein concentration of the fibrin matrix itself.

The detailed molecular basis of the susceptibility effects occurring in samples of DeoxyHb and MetHb is unclear. Gomori et al. [4] ascribed the phenomena to diffusion of water molecules across the red cell membrane to regions of different bulk magnetic susceptibility (portrayed graphically in reviews by Gomori and Grossman [18] and Janick et al. [19]). Gillis and Koenig [20] have suggested that water protons simply diffusing through field gradients adjacent to red cells may account for the phenomena, while Endre et al. [21] suggest the importance of both intracellular and extracellular gradients. Our data do not allow us to distinguish between these two possibilities.

In summary, our study attempted to separate the components of signal intensity in acute and subacute hemorrhage. It emphasizes the importance of normalizing for protein concentration in assessing the effects of paramagnetic forms of hemoglobin. The isointensity of acute hematomas relative to brain parenchyma on short TR/short TE images can be explained by the increased protein concentration of DeoxyHb with little or no PEDD-PRE. The marked hyperintensity of subacute hematomas reflects the superimposed large T1 shortening effect due to PEDD-PRE produced by the high-spin ferric heme of MetHb. The profound hypointensity of acute and early subacute hemorrhages on long TR/long TE images is a function predominantly of the susceptibility effects of intracellular DeoxyHb or intracellular MetHb. The increased protein concentration also plays a role. The increase in signal intensity of subacute hematomas with time on long TR/long TE images reflects first the lysis of the MetHb-containing RBCs followed by breakdown of the hemoglobin and decrease in protein concentration. The PEDD-PRE effects of MetHb, while significant for T1 shortening, are relatively unimportant for T2 shortening.

REFERENCES

1. Gomori JM, Grossman RI, Goldberg HI, Zimmerman RA, Bilaniuk L. Intracranial hematomas: imaging by high-field MR. *Radiology* **1985**;157:87–93
2. Sipponen JT, Sepponen RE, Sivula A. Nuclear magnetic resonance (NMR) imaging of intracerebral hemorrhage in the acute and resolving phases. *J*

Comput Assist Tomogr **1983**;7:954–959
3. Thulborn KR, Waterton JC, Matthews PM, Radda GK. Oxygenation dependence of the transverse relaxation time of water protons in whole blood at high field. *Biochim Biophys Acta* **1982**;714:265–270
4. Gomori JM, Grossman RI, Yu-Ip C, Asakura T. NMR relaxation times of blood: dependence of field strength, oxidation state and cell integrity. *J Comput Assist Tomogr* **1987**;11:684–690
5. Hayman LA, Taber KH, Ford JJ, Saleem A, Gurgun M, Bryan RN. Effect of clot formation and retraction on spin-echo MR images of blood: an in vitro study. *AJNR* **1989**;10:1155–1158
6. Bradley WG, Schmidt PG. Effect of methemoglobin formation on the MR appearance of subarachnoid hemorrhage. *Radiology* **1985**;156:99–103
7. Asakura T. Heme–spin label studies of hemoglobin. *J Biol Chem* **1974**;249:4495–4503
8. Koenig SH, Schillinger WE. Nuclear magnetic relaxation dispersion in protein solutions. *J Biol Chem* **1969**;244:6520–6526
9. Fullerton GD, Finnie MF, Hunter KE, Ord VA, Cameron IL. The influence of macromolecular polymerization on spin-lattice relaxation of aqueous solutions. *Magn Reson Imaging* **1987**;5:353–370
10. Bloembergen N, Purcell EM, Pound RV. Relaxation effects in nuclear magnetic resonance absorption. *Phys Rev* **1948**;73:679–712
11. Hallenga K, Koenig SH. Protein rotational relaxation as studied by solvent 1H and 2H magnetic relaxation. *Biochemistry* **1976**;15:4255–4264
12. Dickerson RE, Geis I. *Hemoglobin: structure, function, evolution and pathology*. Menlo Park, CA: Benjamin/Cummings, **1983**:20–60
13. Wolf GL, Burnett KR, Goldstein EJ, Joseph PM. Contrast agents for magnetic resonance imaging. In: Kressel HY, ed. *Magnetic resonance annual 1985*. New York: Raven, **1985**:231–266
14. Brindle KM, Brown FF, Campbell ID, Grathwohl C, Kuchel PW. Application of spin-echo nuclear magnetic resonance to whole-cell systems. *Biochem J* **1979**;180:37–44
15. Fabry ME, San George RC. Effect of magnetic susceptibility on nuclear magnetic resonance signals arising from red cells: a warning. *Biochemistry* **1983**;22:4119–4125
16. Clark RA, Watanabe AT, Bradley WGJ, Roberts JD. Acute hematomas: effects of deoxygenation, hematocrit, and fibrin-clot formation and retraction on T2 shortening. *Radiology* **1990**;175:201–206
17. Hayman LA, Ford JJ, Taber KH, Saleem A, Round ME, Bryan RN. T2 effect of hemoglobin concentration: assessment with in vitro MR spectroscopy. *Radiology* **1988**;168:489–491
18. Gomori JM, Grossman RI. Head and neck hemorrhage. In: Kressel HY, ed. *Magnetic resonance annual 1987*. New York: Raven, **1987**:71–112
19. Janick PA, Hackney DB, Grossman RI, Asakura T. In vitro modeling of the MR appearance of cerebral hemorrhage. *Magn Reson Q* **1991**;7:57–76.
20. Gillis P, Koenig SH. Transverse relaxation of solvent protons induced by magnetized spheres: application to ferritin, erythrocytes, and magnetite. *Magn Reson Med* **1987**;5:323–345
21. Endre ZH, Kuchel PW, Chapman BE. Cell volume dependence of 1H spin-echo NMR signals in human erythrocyte suspensions. The influence of in situ field gradients. *Biochim Biophys Acta* **1984**;803:137–144